



# Automatic Segmentation by Improved Threshold and Classification by Intelligent Deep Learning Techniques for Lung CT Images Cancer Detection

Ms. HajaBanu Shaikh Mohammed Essa<sup>1\*</sup>, Ms. Zeba Khan<sup>2</sup>

<sup>1</sup>Lecturer, Computer department, Applied College, Jazan University, Jazan, Kingdom of Saudi Arabia, 45142.

Email: hshaikh@jazanu.edu.sa

<sup>2</sup>Lecturer, Computer department, Applied College, Jazan University, Jazan, Kingdom of Saudi Arabia, 45142. zabumazeedullah@jazanu.edu.sa

**Citation:** Ms. HajaBanu Shaikh Mohammed Essa, Ms. Zeba Khan,\_(2024), Automatic Segmentation by Improved Threshold and Classification by Intelligent Deep Learning Techniques for Lung CT Images Cancer Detection, *Educational Administration: Theory and Practice* 30(5), 1518-1530  
Doi: 10.53555/kuey.v30i5.3114

## ARTICLE INFO

## ABSTRACT

Past decades show the failures of lung cancer detection. Lung cancer is the most agonizing disease for humans and many of them do not get cured until the proper treatment [13]. Deep learning Techniques provide an efficient way for a radiologist to analyse the lung images properly and open the right path for accurate Segmentation and Classification. This paper proposed automatic segmentation by improved thresholding technique and evaluated by Dice similarity coefficient, Structure Similarity Index (SSIM), and Feature similarity Index (FSIM). Feature extracted by GLCM for classification and Classified by Neuro-fuzzy classification and RESNET 50 and compared these results with previous research by evaluation metrics Accuracy, Area under the ROC Curve, Sensitivity, Precision, and F1 Score and recommend better classification techniques for lung CT images. This model experiments with the images of the LIDC-IDRI dataset and achieves a 98.99 % Dice similarity coefficient, SSIM as 99%, FSIM as 97.11% for segmentation and classification achieves Accuracy as 99.78%, Area under the ROC Curve as 99.27%, Sensitivity as 99.13%, Precision as 99.01%, and F1 Score as 99.76%. This model suggests a better preprocessing technique denoising autoencoder for medical images and improved dice similarity coefficient for automatic segmentation of lung CT images and also reduce the model loss of RESNET50 in classification of lung CT image classification and attain improved result than [7].

**Keywords:** Segmentation, Feature extraction, Classification, RESNET-50, Evaluation metrics.

## 1. Introduction

Lungs are natural air filter which improves the healthy life of humans and any problem in the lungs leads to a lot of problems, and diseases. Timely identification and prediction of diseases save human lives. In radiology Lung, CT images greatly help the doctors than lung X-Ray images.

It is easy to process but proper usage of techniques only provides better prediction of diseases. The development of machine learning and deep learning algorithms strongly influence the medical world [14], [15]. Particularly deep learning algorithms give a strong foundation for image processing.

The nature of Lung CT images gets affected by environmental conditions, lenses, electrical fluctuations, etc. (problem). Proper preprocessing techniques lead to expected segmentation and classification (overcome problem). This paper mainly focus to analyse the performance of denoising autoencoder preprocessing technique for segmentation and classification and identify the impact of it in result of segmentation and classification. As a result this experiment observes a denoising autoencoder is increase the performance of segmentation and classification.

## 2. Literature Review

Javeed et al., Proposed a new method of hybrid neuro-fuzzy for segmentation. The result of Tumor pixel detection was compared with old methods and found the proposed method achieved 97.3% in tumor cell detection and segmentation is minimum while compared to old methods [1]. Thamilarasi et al developed an Automatic segmentation method for lung chest X-ray images and experiment with mean and standard deviation for RGB channel and achieved dice similarity before applying the filter as 79.71% and after applying the filter as 79.73% and recommend green channel based automatic threshold segmentation [2]. Himansu developed a linguistic Neuro-Fuzzy with Feature Extraction model for classification which is named LNF-FE, LNF-PCA, and eight benchmark datasets utilized for testing and validation. In this paper, PCA is used to reduce the unwanted features and 2.32%, 0.056%, 2.71%, 3.12%, 3.7%, 4.65%, and 2.54% features were reduced from datasets and reported both models to work well for classification [3]. Ashish et al., build a new neuro-fuzzy classification system and experimentation was carried out with 4 benchmark datasets and remote sensing images. For small datasets also this system performs well and for PHONEME dataset accuracy attained 80.09%, for BLOCKS dataset accuracy attained 94.61%, for SATEMAT dataset accuracy attained 82.10% [4]. Thamilaasi et al. experimented with the Canny with morphology and Thresholding technique based segmentation for lung Chest X-Ray images. Jaccard similarity method utilized for performance evaluation and record accuracy of Canny with Morphological segmentation as 76% and accuracy of Thresholding segmentation as 80%. This experiment suggests threshold-based segmentation is better than another one [5]. Peng et al., experimented ResNet 50 model for three different datasets from 562 patients of Nan Fang hospital, 89 patients of Zhu Hai hospital, and 138 patients of Sun Yet-Sen university which considers patient's responses and achieved an accuracy of 84.3%, 85.1%, 82.8% respectively and suggest ResNet-50 suitable for classification [6]. Abhir et al., created modified AlexNet (MAN) to find Lung abnormalities in Chest X-Ra images and Lung CT images. The proposed model MAN achieves >96% accuracy than other DL models and the model MAN with SVM achieves an accuracy of 86.4% and MAN achieved >97.2% accuracy for classification [7]. Moffy et al. developed an automated lung cancer detection system and find morphological operations produced an acceptable result for segmentation and Artificial Neural Network produced acceptable accuracy for classification and an accuracy rate of nearly 92% [8]

## 3. Dataset

LIDC-IDRI dataset was used for the experiment [16]. It provides the location and location of lung nodules. It contains the details of Nodules  $\geq 3$ , Nodules  $<3$ , Non-nodules  $\geq 3$ . nodule sizes are categorized as 8, 2, 43. The dataset contains 1,010 Lung CT cases which contain 1,018 slices. Link for dataset <https://wiki.cancerimagingarchive.net/display/Public/LIDC-IDRI>. The following figure shows the sample images in the dataset.



Figure 1. LIDC- IDRI Sample Images

## 4. Methodology

This section presents the overall methodology of this paper. First, preprocessing techniques have been utilized to remove noises. Secondly, implement an improved threshold for segmentation, Thirdly Feature extraction is established by a few features of GLCM, Fourth classification is done by Neuro-Fuzzy Classifier and deep learning algorithm RESNET-50. The following figure shows the block diagram of the overall methodology.

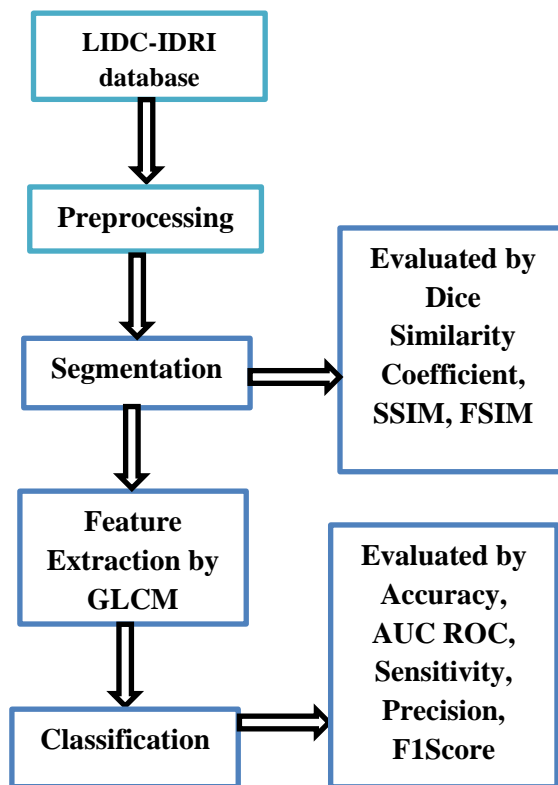


Figure 2. Overall Methodology

**4.1. Preprocessing**

Performance of segmentation and classification model affected by the redundant, noisy, unrelated information in the image dataset. In image processing quality of the image can be improved by preprocessing techniques [17], [18]. In this paper denoising, autoencoder and histogram equalization are utilized for preprocessing.

Denoising autoencoder is one of the leading preprocessing techniques for deep learning. In this paper it is experimented as preprocessing method for lung CT images. Denoising Autoencoders simply add (salt and pepper) noise to the image to keep dominant features. Thereby minimizing the loss function between noisy input and output.

Existing image preprocessing method Histogram equalization is used to improve the contrast of the image. It mainly concentrates on the intensity values of the image. Both techniques role their part and support the result of segmentation and classification [17] [18].

Following figure shows the result of preprocessing

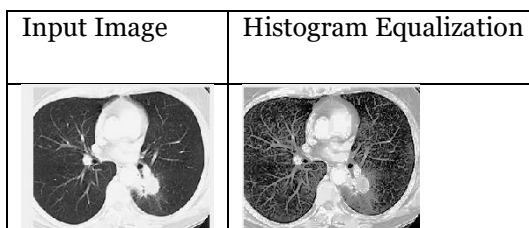


Figure 3. Preprocessing by Histogram Equalization

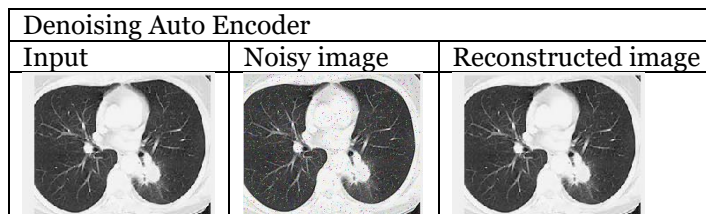


Figure 4. Preprocessing by Denoising Auto Encoder

**4.2. Segmentation**

Segmentation is the activity of breakdown the image into more segments. Based on the nature of the image various segmentation algorithms were adopted for an experiment. Segmentation focuses on meaningful regions, linear structures like lines, curves, shapes like circles, eclipses, etc. It analyses each pixel based on

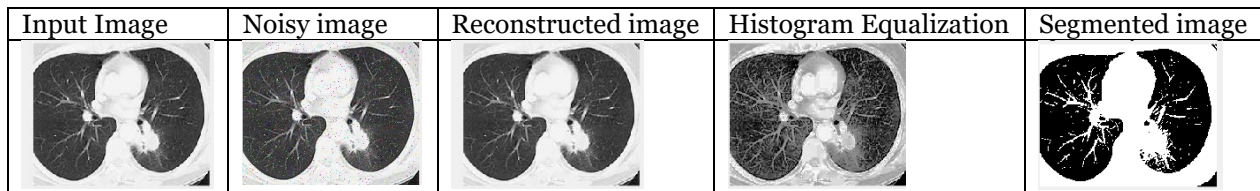
similarity criteria of intensity, histogram features, colour, texture, etc. Automatic segmentation of lung CT images were previously experimented by many researchers and this paper also tried it with mean and standard deviation based threshold [12]. Resulting image from the preprocessing used for segmentation.

#### 4.2.1 Segmentation by Improved Threshold

In this experiment, the threshold is used for segmentation and it normally works based on the intensity level. Threshold-based segmentation is a basic and well-known algorithm for segmentation. Simple selection of threshold values in binary images easily produced segmentation. The threshold value (T) decides the foreground and background segmentation of the image. In segmentation  $<T$  results black and  $>T$  results white. It is difficult to fix a common threshold for Lung CT images, this experiment used three different values to fix the threshold. Improved threshold [2, 5] used for segmentation and it includes the following steps

1. A greyscale image was taken as input.
  2. Preprocessing is done by denoising Autoencoders.
  3. Contrast-enhanced by histogram equalization.
  4. Mean and Standard deviation are used to fix the threshold of the image.
  5. Finally, the segmentation portion gets by binarization.
- The following figure shows the sample image of segmentation by Improved Threshold.

**Figure 5 Segmentation by Improved Threshold**



#### 4.2.2 Evaluation metrics for segmentation

Following metrics are used to measure the performance of improved threshold segmentation and the Dice similarity coefficient achieves 98.99 %, SSIM achieves 99.01%, FSIM achieves 96.34%.

- **Dice Similarity Coefficient**

It is used to identify the similarity between experimental segmented images and ground truth images. It is easily calculated by Dice (bw1, bw2).

- **Structure Similarity Index (SSIM)**

SSIM index focuses on the luminance, contrast, and structural aspects of an image and it has been calculated by the dot product of these features.

$$SSIM(a, b) = [l(a, b)]^\alpha \cdot [c(a, b)]^\beta \cdot [s(a, b)]^\gamma \quad (10)$$

The luminance, Contrast, and Structure of an image are expressed as follows

$$l(a, b) = \frac{2\mu_a\mu_b + c_1}{\mu_a^2 + \mu_b^2 + c_1} \quad (1)$$

$$c(a, b) = \frac{2\sigma_a\sigma_b + c_2}{\sigma_a^2 + \sigma_b^2 + c_2} \quad (2)$$

$$s(a, b) = \frac{\sigma_{ab} + c_3}{\sigma_a\sigma_b + c_3} \quad (3)$$

$\mu_a, \mu_b$  : Local means

$\sigma_a, \sigma_b$  : Standard Deviation

$\sigma_{ab}$  : Cross Covariance for images a & b. The value of SSIM considered between 0 & 1 normalized scale.

- **Feature Similarity Index Matrix (FSIM)**

It works based on Phase congruency (PC) and Gradient Magnitude (GM). PC of images denoted by  $PC_1, PC_2$ . The similarity of images can be calculated as

$$Spc = \frac{2PC_1PC_2 + T_1}{PC_1^2 + PC_2^2 + T_1} \quad (4)$$

GM of images expressed as  $G_1, G_2$  and Similarity of images calculated as

$$Sc = \frac{2G_1G_2 + T_2}{G_1^2 + G_2^2 + T_2} \quad (5)$$

FSIM computed by multiplication of these two measures.

$$S_L(x) = [S_{PC}(x)]^\alpha \cdot [S_C(x)]^\beta \quad (6)$$

### 4.3. Feature Extraction

It is also one of the dimensionality reduction method. Large volume of data can be easily reduced for further processing. In this experiment GLGM features such as energy, entropy, contrast, correlation, and homogeneity have been utilized.

**Contrast:** Contrast calculated by sum of square variance. Scale of local texture decides the value of contrast.

$$\text{Contrast} = \sum_{i,j=0}^{N-1} P_{ij}(i - j)^2 \quad (7)$$

**Energy:** Orderliness of image calculated by energy and provide sum of square elements of GLCM.

$$\text{Energy} = \sum_{i,j=0}^{N-1} (P_{ij})^2 \quad (8)$$

**Entropy:** Wrong order of pixels identified by entropy

$$\text{Entropy} = \sum_{i,j=0}^{N-1} -\ln(P_{ij})P_{ij} \quad (9)$$

**Correlation:** It calculates the correlation of pixel in the entire image.

$$\text{Correlation} = \sum_{i,j=0}^{N-1} P_{ij} \frac{(i-\mu)(j-\mu)}{\sigma^2} \quad (10)$$

**Homogeneity:** It focus smoothness distribution of the image. If homogeneity is high, contrast is low.

$$\text{Homogeneity} = \sum_{i,j=0}^{N-1} \frac{P_{ij}}{1+(i+j)^2} \quad (11)$$

### 4.4 Classification

Locating similar categories of the pixel into a group or class is called image classification. Feature sets and learning techniques help with proper classification. Various class attributes are used as features. Classifiers are used to identify the relationship between data and classes. The complexity and limitations of previous mechanisms are largely due to the lacking of an effective way of defining the boundaries among clusters or classes. In this experiment classification was carried out by Neuro-Fuzzy Classifier and ResNet50. This ResNet50 architecture previously experimented by some researchers [11] but in this experiment this algorithm utilized to check the performance of classification after preprocessing with denoising autoencoder.

#### 4.4.1 Neuro-Fuzzy Classification

Neural network and fuzzy logic combined to create an effective model which is called a neuro-fuzzy model. It works based on fuzzy set relations and membership function values of each set. Neuro-fuzzy model activation functions, connection weights, and propagation functions are different from normal neural networks. Neuro-fuzzy system works based on fuzzy sets. It has three feed-forward layers one represents the input layer, the second represents the middle layer, and the third layer represents the output layer. Neuro-fuzzy system is interpreted as a system of fuzzy rules and sometimes training data utilize prior features. The following figure shows the implementation model of the Neuro-fuzzy Classifier and 500 images of Lung CT images were used for classification.

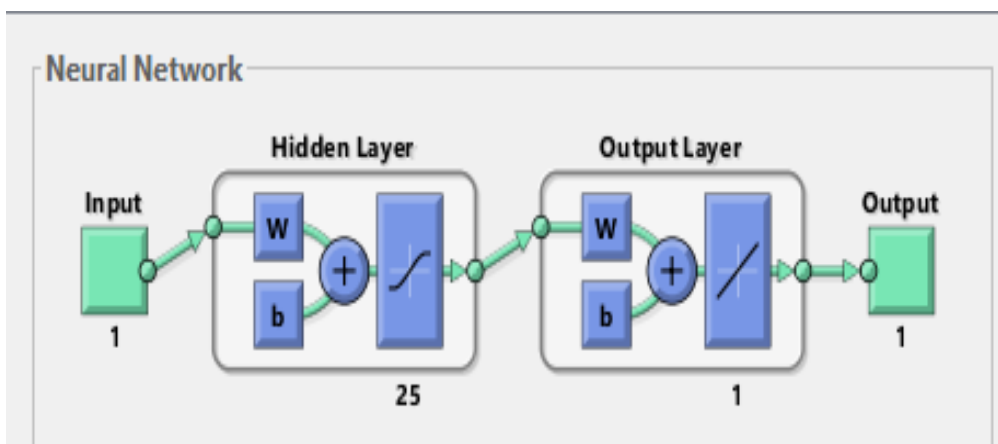


**Figure.6 Implementation model of Neuro-fuzzy Classifier**

#### 4.4.2. ResNet50

Deep learning architectures greatly support the diagnosis of medical images [9], [10], [11]. Due to model loss many algorithms not able to provide successful results. To overcome the problem of model loss this experiment used denoising autoencoder for preprocessing and execute the processed for classification. Residual networks are shortly termed as ResNet. This model strongly supports the classification problem. It has 50 neural networks with many variants. To overcome the deep learning problem of Vanishing or gradient ResNet has been created thereby improving the accuracy of models. This type of network worked on the concept of skip connections. Its architecture same as ResNet32 and 3-layer bottleneck block is used instead of 2-layer blocks in ResNet 32.

Skip connections avoid the problem in layer architecture, it automatically skips the regularization thereby reducing the issues of vanishing and exploding gradient.

ResNet-50 model builds with 5 stages with convolution block and identity block. Both blocks have 3 convolution layers. The ResNet-50 consists of 23 million trainable parameters. The following figure shows the basic model of ResNet-50.

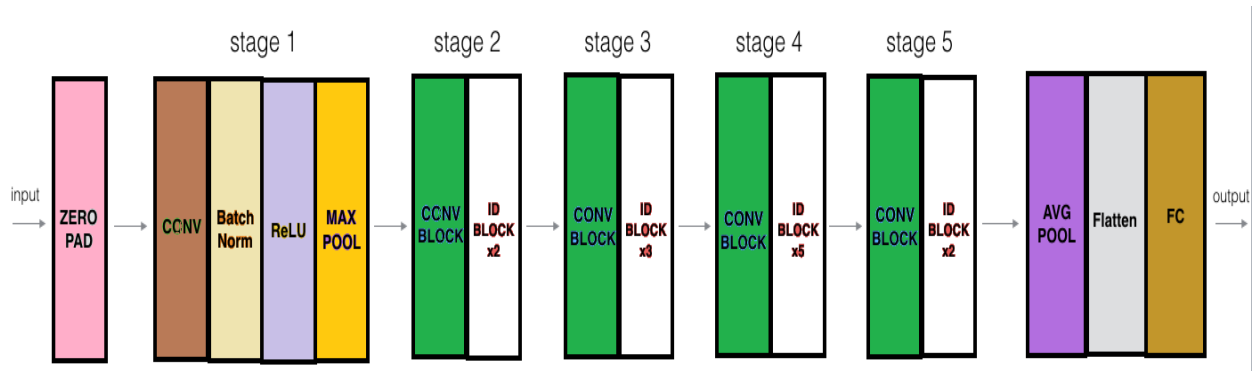


**Figure.7 ResNet-50 Model**

In this experiment, ResNet-50 was executed with

- Zero padding: pads the input with (3,3)
- Convolution layers are used to capture the dominant features in the image
- Batch Normalization normalizes the every input layer and increases the performance
- ReLu Activation function operates in hidden layers and propagates the errors.
- Max pooling is used for dimensionality reduction
- Finally full connected layer work with Average pooling.
- Flatten does not have any parameters. For classification also limited images of Lung CT images were used.

The following figure shows the layer model of ResNet-50(a few layers).

Model: "ResNet50"

Layer (type)	Output Shape	Param #	Connected to
input (InputLayer)	[(None, 64, 64, 3)]	0	o
zero_pad (ZeroPadding2D)	(None, 70, 70, 3)	0	input[o][o]
conv1 (Conv2D)	(None, 32, 32, 64)	9472	zero_pad[o][o]
b_conv1 (BatchNormalization)	(None, 32, 32, 64)	256	conv1[o][o]
act (Activation)	(None, 32, 32, 64)	0	b_conv1[o][o]
max_pooling (MaxPooling2D)	(None, 15, 15, 64)	0	act[o][o]
res_branch2 (Conv2D)	(None, 15, 15, 64)	4160	max_pooling[o][o]

**Figure .8 Layer model of ResNet-50**

Residual Block Identity mappings in ResNet-50 are as follows

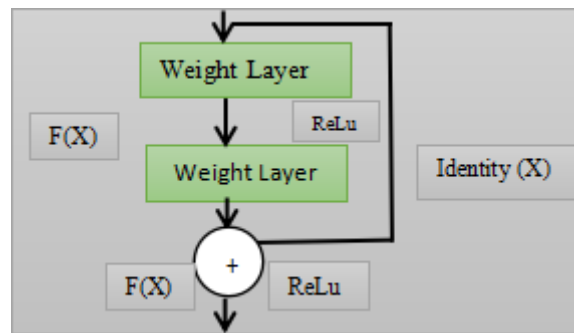


**Figure .9 Residual Block**

This model explicitly allows the layers to fit the residual mapping and termed  $G(X)$  and also allows another mapping non-linear layers to fit  $F(X)=G(X)-X$ , The equation for original mapping is  $G(X)=F(X)+X$ . This shortcut identity mapping saves the computational time.

Working methodology of ResNet-50 as follows

- 1.1<sup>st</sup> layer:  $7*7$  and 64 different kernels with stride=2
2. Max pooling with stride=2
3.  $1*1, 64$  kernel,  $3*3, 64$  kernel, and  $1*1, 256$  kernel these 3 layers are repeated 3 times so a total of 9 layers
4.  $1*1, 128$  kernel,  $3*3, 128$  kernel, and  $1*1, 512$  kernels these 3 layers are repeated 4 times so a total of 12 layers
5.  $1*1, 256$  kernel,  $3*3, 256$  kernels, and  $1*1, 1024$  kernel these 3 layers are repeated 6 times so a total of 18 layers
6.  $1*1, 512$  kernels,  $3*3, 512$  kernels,  $1*1, 2048$  kernel these 3 layers repeated 3 times so totally 9 layers
7. Final layer average pooling + 1000 nodes of full connected layer +softmax function. All these layers produce the 50 convolution layers (48 convolution layers + 1 max pooling layer+1 average pooling layer) of ResNet-50.

#### 4.4.3 Evaluation metrics

Evaluation metrics used for classification are

**Accuracy:** It is a basic metric used by Machine learning and deep learning models. It is a ratio between actual pixel prediction and architecture pixel prediction. It is calculated as follows

$$\text{Accuracy} = \frac{TP+TN}{TP+TN+FP+FN} \quad 12$$

**The area under curve ROC:** ROC stands for Receiver Operating Characteristics Curve. It is used to measure the capability of classification models and also used to select a threshold for the classifier. The area under the curve is used for binary classification problems. AUC supports classifiers to differentiate classes and is also used as a summary of the ROC curve.

**Precision:** It predict the number of correct positive predictions. It is calculated as follows

$$\text{Precision} = \frac{\text{True Positive}}{\text{True Positive} + \text{False Positive}} \quad 13$$

**Sensitivity:** Sensitivity also termed as Recall. It ia calculated as follows

$$\text{Sensitivity} = \frac{\text{True Positive}}{\text{True Positive} + \text{False Positive}} * 100 \quad 14$$

**F1 Score:** It is termed as harmonic mean of precision and recall

$$\text{F1 Score} = 2 * \frac{\text{Precision} * \text{Recall}}{\text{Precision} + \text{Recall}} \quad 15$$

## 5. Result and Discussion:

### Contribution

- This research used denoising autoencoder for preprocessing to enhance the image. As a result of this loss of total model is reduced.
- In previous research there is no automatic segmentation by mean and standard deviation based threshold for lung CT images [2] and this algorithm reduce the time of segmentation.
- This research experiment with neuro-fuzzy classifier, ResNet-50 for classification and results shows that denoising autoencoder reduce model loss and overall performance of ResNet classification improved while compared to the state of art method [7].
- The Experimented ResNet 50 achieves Accuracy 99.78 , Precision 99.01, Sensitivity 99.13, F1 Score 99.76 than previous experiment [7] Accuracy 86.07 , Precision 90.30, Sensitivity 88.97, Specificity 80, F1 Score 89.63.
- This experiment improves the accuracy and reduce the loss of the classifier.

The following Table 1 shows the before and after preprocessing of image with very low MSE loss

**Table 1. MSE loss: Before and after preprocessing**

DAE MSE Loss Values	
Before	After
0.031	0.025

Following table 2 shows the values of Improved Threshold segmentation evaluation metrics.

**Table 2. Improved Threshold segmentation evaluation metrics**

Evaluation Metrics	Values (%)
Dice Similarity Coefficient	98.99
SSIM	99.01
FSIM	97.11

Following figure 10 shows the graphical representation of Improved Threshold segmentation evaluation metrics comparison.

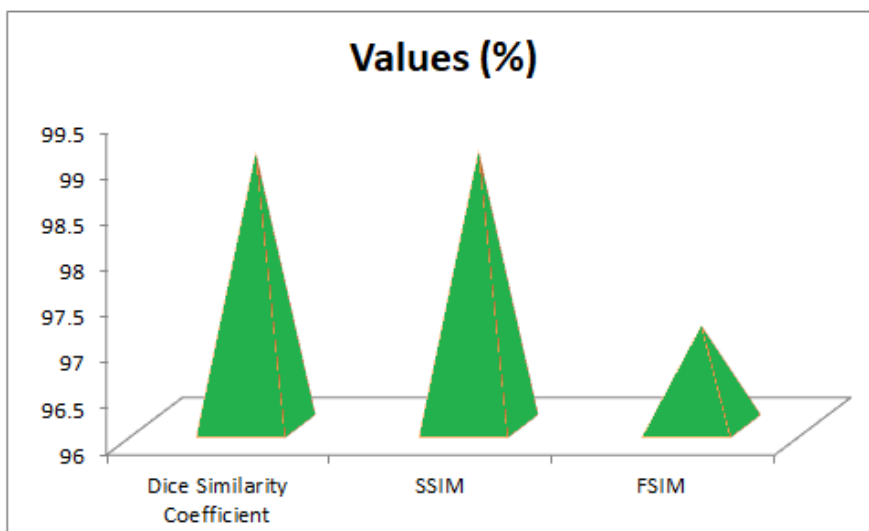


**Figure .10 Comparison of Improved Threshold segmentation evaluation metrics.**

The metrics used to evaluate improved threshold segmentation are the dice similarity coefficient, SSIM, and FSIM. Figure 10 shows that the values of these three metrics are better for the suggested model. Because of the recommended work's automated segmentation technique. This automated segmentation is based on a threshold value calculated from the mean and standard deviation values. The segmentation procedure concentrates exclusively on the meaningful region of the lung CT images. These three measures attain higher values by just evaluating the meaningful regions of the images.

The following table 3 shows the evaluation metric table for segmentation (500 images)

**Table 3. Improved Threshold Segmentation**

Input Image	Segmentation by improved Threshold	Dice similarity coefficient	SSIM	FSIM
		98.99 %	99.01%	97.11%

The following diagram shows the best training performance of the Neuro Fuzzy Classifier

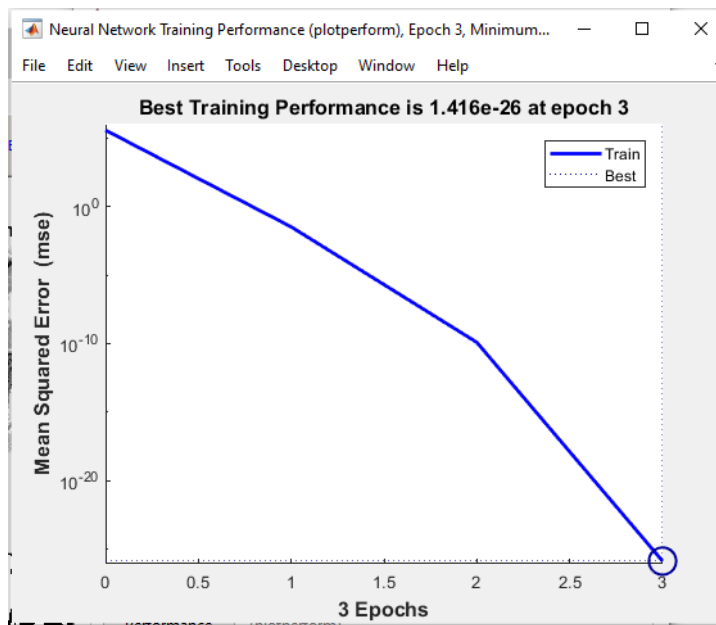


Figure .11 Best training performance of Neuro-Fuzzy Classifier

The following diagram shows the training Regression of the Neuro-Fuzzy Classifier

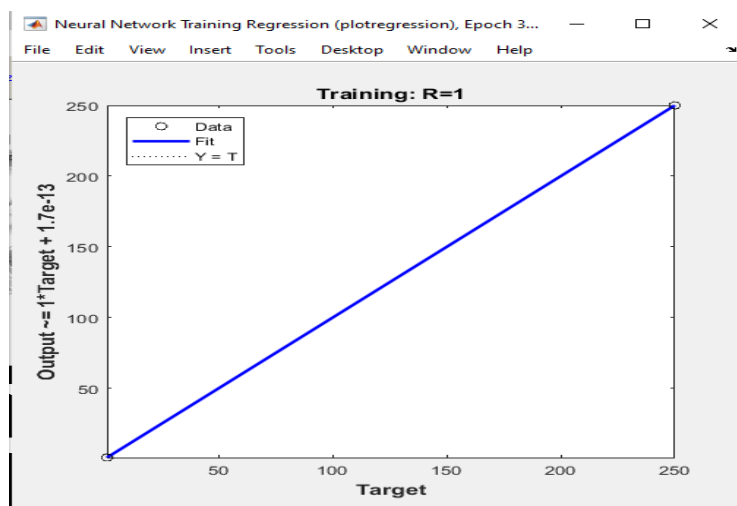


Figure 12. Training Regression of Neuro-Fuzzy Classifier

The following figure shows the Training state of the Neuro-Fuzzy Classifier

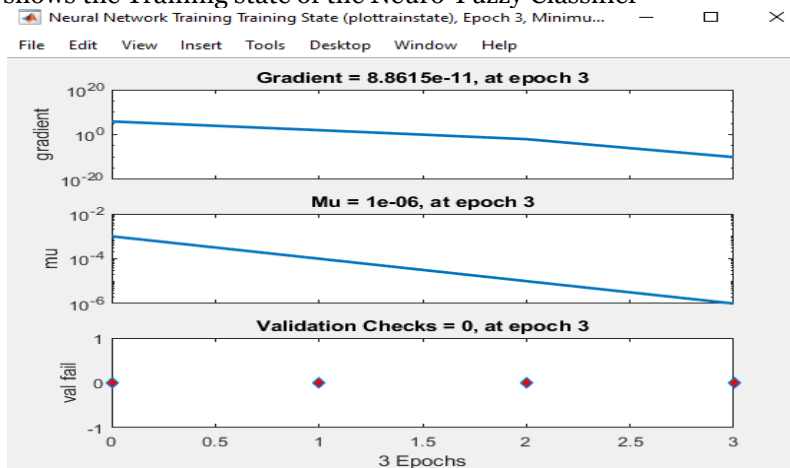


Figure 13. Training state of Neuro-Fuzzy Classifier

The following table shows the previous models [7] and the proposed method evaluation metric comparison.

**Table 4. Comparison of previous models [7] and proposed method evaluation metric**

Classifiers	Accuracy (%)	Precision (%)	Sensitivity (%)	F1 Score
Previous ResNet-50	86.07	90.30	88.97	89.63
Previous MAN SVM	86.47	92.20	88.06	90.08
Proposed Neuro-Fuzzy Classifier	93.63	93.10	93.24	93.51
Proposed ResNet-50	99.78	99.01	99.13	99.76

The following figure 14 shows the graphical representation of previous models (10) and the proposed method evaluation metric.

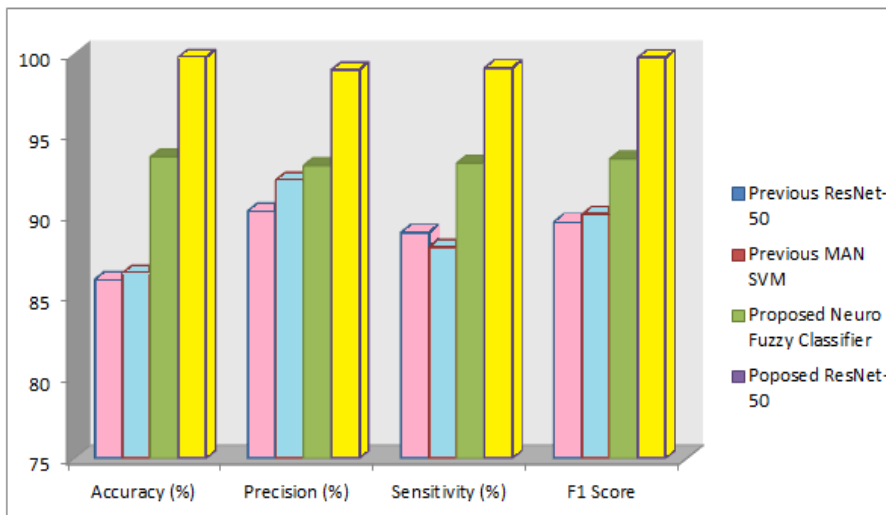


**Figure 14. Graphical representation of previous models (10) and proposed method evaluation metric.**

The following table shows the Evaluation metrics used to measure the Performance of the Neuro-fuzzy classifier and ResNet-50 as follows

**Table 5. Evaluation metrics used to measure the Performance of the Neuro-fuzzy classifier and ResNet-50**

Classifiers	Accuracy (%)	Precision (%)	Sensitivity (%)	F1 Score (%)	AOUROC (%)
Proposed Neuro-Fuzzy Classifier	93.63	93.10	93.24	93.51	93.32
Proposed ResNet-50	99.78	99.01	99.13	99.76	99.27

The following figure 15 shows the graphical representation of Evaluation metrics used to measure the performance of the Neuro-fuzzy classifier and ResNet-50.

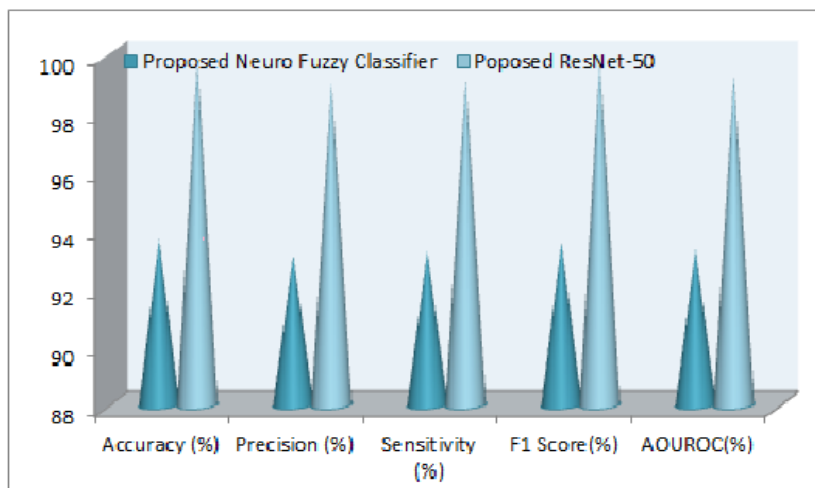


**Figure 15. Performance of Neuro-fuzzy classifier and ResNet-50 measured by the evaluation metric**

Figures 14 and 15 show that the precision, accuracy, sensitivity, and ROC values of the proposed model are greater than those of the existing model. Because ResNet topologies require a large number of convolution layers. This layer is intended to automatically collect the main characteristics of lung CT images without the need for human involvement. The automated feature extraction simplifies and improves the categorization process. Another issue with deep learning is the vanishing gradient problem, which is connected to model accuracy. These issues were solved by the skip connections in the suggested paradigm. It automatically skips regularisation, avoiding the problem of vanishing and exploding gradients in layer design. As a result, the model's accuracy increased over previous models.

The following table 6 shows the improvement of result after preprocessing with denoising autoencoder.

**Table 6. MSE Loss after Preprocessing**

DAE MSE Loss Values	
Before preprocessing	After classification
0.031	0.022

The following diagram shows the graphical representation of improvement of result before & after preprocessing classification with denoising autoencoder.

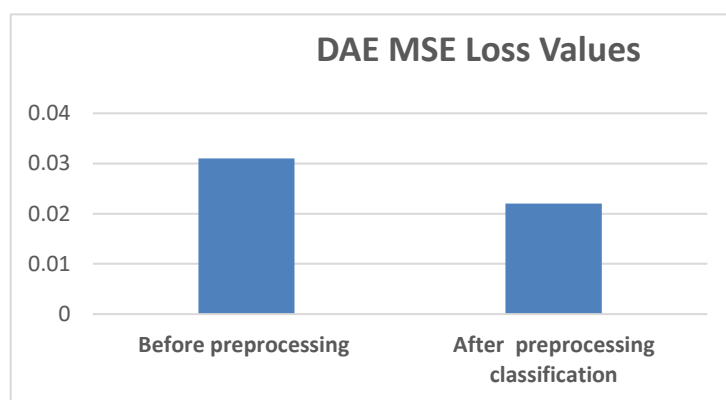


**Figure 16. Before & after preprocessing classification**

The following table 7 shows the improvement of result after preprocessing with denoising autoencoder.

**Table 7. MSE Loss before & after Preprocessing**

DAE MSE Loss Values			
Before preprocessing	After preprocessing	After Segmentation	After classification
0.031	0.025	0.024	0.022

The following diagram shows the graphical representation MSE Loss before & after preprocessing with denoising autoencoder.

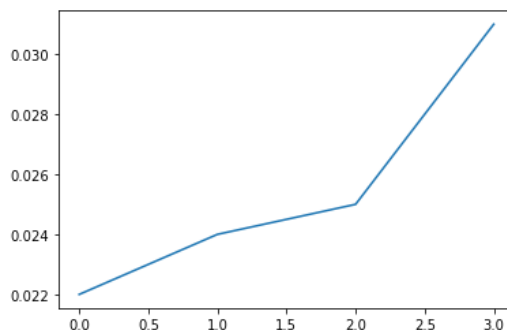


**Figure 17. MSE Loss before & after preprocessing (Segmentation & Classification)**

Figures 16 and 17 show that the MSE loss value of the proposed model is quite low after preprocessing. However, the loss value is large before preprocessing because segmenting and classifying pictures containing noisy data, duplicate information, and irrelevant information is challenging. With this information, the classification process may be useless, result in incorrect classification, large loss values, and low accuracy.

The suggested approach avoids these issues by utilising the denoising autoencoder. This reduces noise information and improves image quality, making it ideal for successful categorization.

### Findings:

- The above results shows the denoising auto encoder bitterly improve the performance of Classification due to minimum MSE Loss 0.022.
- This experiment recommends evaluation metric SSIM for improved threshold automatic segmentation than dice similarity coefficient and FSIM.
- For classification this experiment suggests ResNet-50 which attains higher result than the previous experiment result [7].
- This experiment also suggest Accuracy and F1 Score suitable evaluation metrics for classification.

## 6. Conclusion

Lung segmentation and classification is a challenging and time-consuming process for researchers. The main goal of this experiment is to propose a low cost and less time considering segmentation and classification model for Lung CT images. After preprocessing with denoising autoencoder the experimented Improved Threshold for Automatic Segmentation achieves Dice similarity coefficient of 98.99 % , SSIM of 99%, and FSIM of 97.11% for Automatic Segmentation. Classification carried out by Neuro-Fuzzy Classifier and ResNet-50 and the performance evaluation achieved by Accuracy as 99.78%, Area under the ROC Curve as 99.27%, Sensitivity as 99.13%, Precision as 99.01%, and F1 Score as 99.76% for ResNet-50 and Accuracy as 93.63%, Area under the ROC Curve as 93.32 % , Sensitivity as 93.24 % , Precision as 99.01%, and F1 Score as 93.51 % for Neuro-Fuzzy Classifier. This experiment finds ResNet-50 is suitable for Lung CT image classification and it achieved improvement over the old method [7]. This experiment used the original architecture of ResNet-50, in the future, it gives a path to experiment with a different number of layers for Lung CT image classification. As a result the whole experiment considerably improve the results in segmentation and classification. This research suggest denoising autoencoder is suitable preprocessing method classification for Lung CT images which meets only 0.022 MSE Loss value for classification by ResNet-50 and it also improve the overall performance of accuracy and which sets a path to all medical images.

## 7. References

1. S.Javeed Hussain, S.Asif Hussain, M.Praveen Raju, D.Satyanarayana,, C.Venkatesh, "Neuro-Fuzzy System for Medical Image Processing"m IEEE, PP.52-55, 2010.
2. V.Thamilarasi and R.Roselin, " Automatic Thresholding for Segmentation in Chest X-Ray Images Based on Green Channel Using Mean and Standard Deviation", International Journal of Innovative Technology and Exploring Engineering (IJITEE) ISSN: 2278-3075, 2019, Vol-8, Iss-8: pp. 695-699.
3. Himansu Dasa, Bighnaraj Naik, H.S.Behra, " Medical disease analysis using Neuro-Fuzzy with Feature Extraction Model for Classification", Informatics in Medical Unlocked, Elsevier, pp. 1-12, 2020.
4. Ashish Ghosh, B.Uma Sankar, "A novel approach to neuro-fuzzy classification", Neural Networks, vol.no:22, pp: 100-109, 2009.
5. Thamilarasi V., Roselin R., Lung Segmentation In Chest X-Ray Images Using Canny With Morphology And Thresholding Techniques. International Journal of Advance and Innovative Research, Vol 6, Issue 1(VII) , pp. 1-7, (2019).
6. Jie Peng, Shai Kang AND Zhengyuan Ning & Hangxia Deng & Jingxin Shen & Yikai Xu & Jing Zhang & Wei Zhao. Xinling Li, Wuxing Gong, Jinhua Huang, "Residual convolutional neural network for predicting response for predicting response of transarterial chemoembolization in hepatocellular carcinoma from CT imaging", European Radiology (Springer), pp.1-12, 2019.
7. Abhir et al., " Deep-Learning framework to detect lung abnormality - A study with chest X-Ray and Lung CT scan images", Pattern Recognition Letters (Elsevier), pp.1-7, 2019.
8. Moffy Vasi, Amita Dessai." Lung Cancer detection system using lung CT image processing", IEEE, .1-5, 2017.
9. Thamilarasi V., Roselin. R., Automatic Classification and Accuracy by Deep Learning Using CNN Methods in Lung Chest X-Ray Image, IOP Conf. Ser.: Mater. Sci. Eng. 1055 012099, 2020.
10. Thamilarasi V., Roselin. R., U-Net: Convolution Neural Network for Lung Image Segmentation and Classification in Chest X-Ray images, INFOCOMP, Vol. 20, No. 1, pp.. 101-108 (2021).
11. Raul Victor Medeiros da Nobrega, Solon Alves Peixoto, Suane Pires P. da Silva, and Pedro Pedose Reboucas Filho, "Lung Nodule Classification via Deep Transfer Learning in CT Lung Images", IEEE 31<sup>st</sup> International Symposium on Compute Based Medical Sstems, E-ISSN: 2372-9198, P.18-21, 2018.
12. M.Afan Jaffar, Ayyaz Hussain, M.Nazir et al., "GA and Morphology based Automated Segmentation of Lungs from CT Scan Images", 2008 Intenational Confence on Computational Intelligence for Modelling Control & Automation, pp.265-270, 2009.

13. R.L.Siegel, K.D.Miller and A.Jemal, “ Cancer statistics 2017”, CA:A Cance Journal for Clinicians , Vol.67, No.1, pp.7-30, 2017.
14. S.G.L.F.Da Silva, O..Da Silva Neto, A.C.Silva, A.C.de Paiva, M.Gattass, “ lung nodules diagnosis based on evolutionary convolutional neural network”, Multimed tools Appl, Vol.76, pp.19039 -19055, 2017.
15. M.F.Seri, B.Lavi, G.Hoff, D.P.Valls, “A deep convolutional neural network for lung cancer diagnostic”, 2018, arXiv:1804.08170v1 [cs.CV].
16. T.G.Armato and Geoffrey McLennan et al. “ The lung image database consortium (LIDC) and image database resource initiative (IDRI): a completed refeence database of lung nodules on CT scans”, Med Phys, Vol.38, No.2, pp.915-931, 2011.
17. Guy Caseneuve, Iren Valova et al., “ Chest X-Ray image preprocessing for disease classification”, 25<sup>th</sup> International conference on knowledge based and intelligent information & Engineering systems, Vol.192, pp.658-669, 2021.
18. A.Giełczyk, A. Marciniak, M.Tarczewska, Z.Lutowski, “ Pre-processing methods in chest X-ray image classification”, PLoS ONE, Vol.17, No.4, 2022. e0265949. <https://doi.org/10.1371/journal.pone.0265949>